Seasonal variation of mercury concentration of ancient olive groves of Lebanon.

Nagham Tabaja[1,2,3], David Amouroux[4], Lamis Chalak[2], François Fourel [5], Emmanuel Tessier [4], Ihab Jomaa [6], Milad El Riachy [7], Ilham Bentaleb [1]

[1] ISEM, Univ Montpellier, CNRS, IRD, Montpellier, France
[2] Faculty of Agronomy, Plant Production Department, The Lebanese University, Dekwaneh, Lebanon
[3] Plateforme de Recherche et d'Analyses en Sciences de l'Environnement (PRASE), Ecole Doctorale de Sciences et Technologie, Université Libanaise, Hadath, Liban
[4] Université de Pau et des Pays de l'Adour, E2S/UPPA, CNRS, Institut des Sciences Analytiques et de Physico-Chimie pour l'Environnement et les Matériaux (IPREM), PAU, France
[5] UMR CNRS 5023 LEHNA, Université Claude Bernard Lyon 1, Villeubanne, France
[6] Department of Irrigation and Agrometeorology, Lebanese Agricultural Research Institute (LARI), P.O. box 287, Zahle, Lebanon
[7] Department of Olive and Olive Oil, Lebanese Agricultural Research Institute (LARI), P.O. box 287, Zahle, Lebanon

Correspondence to: Ilham Bentaleb (Email: ilham.bentaleb@umontpellier.fr, Tel: +33(0) 6 38 61 57 69)

Abstract. This study aimed to investigate the seasonality of the mercury (Hg) concentration of olive trees foliage, an iconic tree of the Mediterranean basin. Hg concentrations of foliage, stems, soil surface, and litter were analyzed on monthly basis in ancient olive trees growing in two groves in Lebanon, Bchaaleh and Kawkaba (1300 and 672 m.a.s.l respectively). A significantly lower concentration was registered in stems (~7-9 ng/g) with respect to foliage (~35-48 ng/g) in both sites with the highest foliage Hg concentration in late winter-early spring and the lowest in summer. It is noteworthy that olive fruits also have low Hg concentration (~7-11 ng/g). The soil has the highest Hg content (~62-129 ng/g) likely inherited through the cumulated litter biomass (~ 63-76 ng/g). A good covariation observed between our foliage Hg time-series analysis and those of atmospheric Hg concentrations available for southern Italy in the western Mediterranean basin confirms that mercury pollution can be studied through olive trees. More precisely, spring sampling is recommended if the objective is to assess the tree's susceptibility to Hg uptake. Our study draws an adequate baseline for Eastern Mediterranean and region with similar climate inventories on Hg vegetation uptake and new studies on olive trees in the Mediterranean to reconstruct regional Hg pollution concentrations in the past and present.

Keywords: Eastern Mediterranean, ancient groves, *Olea europaea* L., mercury pollution, plant tissues, soil and litter

Introduction

Mercury (Hg) is among the most widely distributed potentially toxic metals polluting the Earth (Briffa et al. 2020). It is found as all heavy metals naturally on the Earth's crust reservoir and in the atmosphere through the natural long-term Hg biogeochemical cycle (i.e., volcanic activities, geological weathering). This metal is easily modified into several oxidation states and it can also be spread through many ecosystems (Boening 2000). The natural Hg cycle has been modified due to anthropogenic activities (i.e., mining, smelting, soil erosion due to deforestation, gold extraction, agriculture-fertilizers, manure) (Patra and Sharma 2000). Among natural and anthropogenic Hg emissions, inorganic elemental Hg (Hg(0)) is the most dominant chemical form. It is primarily transferred through the atmosphere by air mass movement and can undergo long-range transport. Because of its high volatility and susceptibility to oxidation, elemental Hg(0) is the predominant form of Hg in the atmosphere that can be accumulated into foliage. This highly diffusive Hg can easily pass biological barriers (i.e. cell membranes, foliage, skin). Mercury has three oxidation states, namely, Hg(0) (elemental mercury), Hg(I) (mercurous), or Hg(II) (mercuric), although Hg(I) mercurous form is not stable under typical environmental conditions and, therefore, is rarely observed. It is likely that the Hg(II) high binding affinities bind covalently with organic groups (Du and Fang, 1983; Clarkson and Magos 2006; Pleijel et al., 2021). The exchange of Hg between the soil and plants is not stable and is variable dependent (e.g. cation-exchange capacity, soil pH, soil aeration, and plant species) (Patra and Sharma 2000).

Forests are known to act as a sink of atmospheric Hg. Plant foliage takes up of Hg deposited on leaf surfaces through the stomata (i.e. Leaf gas exchange) and leaf cuticles (Hanson et al. 1995; Jiskra et al. 2018; Li et al. 2017; Lodenius et al. 2003; Maillard et al. 2016; Rea et al. 2002; Yanai et al. 2020) where it accumulates with minimal mobility and small portions released back into the atmosphere or transferred to other plant organs (Cavallini et al. 1999; Hanson et al. 1995; Li et al. 2017; Lodenius et al. 2003; Schwesig and Krebs 2003). All together these authors contributed to highlight the dynamic role of the foliar surfaces in terrestrial forest landscapes acting as a source or sink dependent on the magnitude of current Hg concentrations. Hanson et al. (1995) suggested a species-specific compensation concentrations (or compensation points) for Hg deposition.

Hg is redistributed to the forest floor through litter and throughfall and hence passes to the soil (Rea et al. 1996). The Hg input through the litter is greater than the input from that of the wet deposition (Wang et al., 2016). Litter has been estimated to constitute 30 to 60 % of the Hg atmospheric deposition in Europe and North America forests (Rea et al. 1996; Blackwell and Driscoll 2015; Zhou et al. 2018). According to Wright et al., (2016) the litter Hg is the dominant pathway in forests where it contributes 53 to 90 % of the dry deposition to the forest.

In terrestrial ecosystem, soil as part of the geological reservoir has naturally the highest Hg reservoir (Obrist et al., 2018; O'Connor et al., 2019) followed by trees (Yang et al., 2018). This Hg is provided by natural geological sources and natural events such as forest fires, volcanic eruptions (Ermolin et al. 2018; Obrist et al. 2018; O′Connor et al. 2019) and anthropogenic sources (UNEP, 2019).

Though variable from year to year, Hg emission to the atmosphere from biomass burning is considered as an important driver of the global Hg biogeochemical cycle (Friedli et al., 2009; De Simone et al., 2015; McLagan et al., 2021; Dastoor et al., 2022). Soil can also release Hg to the atmosphere (Luo et al., 2016; Assad, 2017; Yang et al., 2018; Schneider et al., 2019; Gworek et al., 2020; Pleijel et al., 2021) and also behave as a source of Hg to the plants. Hg of

the soil is is taken up by the roots along with the water , it is translocated to other parts (ie. Stems, Leaves) of the plant using the xylem sap (Bishop et al., 1998; Li et al., 2017). This pathway have been described on several plant species in Hg contaminated sites (Assad et al. 2017). Trees are hence considered as important drivers of Hg exchange between the atmosphere and the soil (Yang et al. 2018). The recent studies on Hg uptake by vegetation have highlighted the importance of the role of different parameters as vapor pressure deficit, soil water content, climatic conditions, date of sampling, leaf mass area, tree functional groups, stomatal conductance, affecting potentially the root uptake of Hg dissolved in soil water and the absorption rate via stomata and eventually the Hg leaf content (Rea et al., 2002; Obrist et al., 2011; Blackwell & Driscoll, 2015; Yang et al., 2018; Wohlgemuth et al., 2021). In polluted sites the soil is the main source of Hg to the vegetation while away from those sites the atmosphere is the most important source (Naharro et al., 2018). The Hg source in foliage varies with respect to the amount of contamination (Hanson et al., 1995).

The studies of the Hg cycle in forest ecosystems show that gaseous elemental Hg(0) is the main source taken up by plants (Bishop et al. 2020; Zhou et al. 2021). Analysis of long term atmospheric Hg(0) and CO_2 concentrations are very informative to understand the role of the vegetation in the global Hg cycle (Jiskra et al., 2018). Emission reduction measures adopted in Europe and North America since the 70s are corroborated by Hg dendrochemistry analysis showing a declining Hg concentration trend from the older to newer tree rings. Indeed, tree ring Hg (dendrochronology) is a powerful archiving tool for atmospheric Hg(0). After Hg(0) oxidation inside the leaves, Hg(II) bind to organic compounds and then is transported to the bole wood via the phloem (Beauford et al., 1977; Lindberg et al., 1979). This is corroborated by the recent study of McLagan et al., (2022) showing the benefit of the stable Hg isotope analysis on dendrochemistry. Several studies have evidenced seasonal variations of the atmospheric Hg(0) contents (ie. in temperate Northern Hemisphere by Jiskra et al., 2018; in Western Mediterranean Basin in South Italy (Martino et al. 2022) with high values in winter and low values in summer. Interinstingly, Jiskra et al., (2018) show also a significant positive correlation between the monthly Hg(0) and CO_2 concentrations. They highlighted a one-month offset in Hg(0) summer time minima happening in September in comparison to the CO_2 minima value occurring in August, this trend is not observed in winter time. The uptake of Hg(0) by the vegetation continues during CO_2 respiration periods during the fall and night when the ecosystem exchange of CO_2 turns from being a sink to becoming a source (Wofsy et al., 1993; Jiskra et al., 2018).

The total gaseous Hg (TGM) in the Mediterranean atmosphere is similar to Northern Europe (1.3 to 2.4 ng m^{-3}) (Kotnik et al. 2014). In the case of a semi-closed sea such as the Mediterranean basin with warm summers, high sea-water evaporation, solar radiations and Hg anthropogenic sources, the Mediterranean Sea acts as a net source of Hg to the global atmosphere (Kotnik et al. 2014) making the Mediterranean an air-pollution emission area (Baayoun et al. 2019; Borjac et al. 2019).

The olive tree (*Olea europaea* L.) is one of the most distinctive Mediterranean agro-ecosystems tree species (Besnard et al., 2013), and is adapted to drought (Sghaier et al. 2019). Considered to be among the oldest trees in the Mediterranean basin, centennial olive trees are still growing in many countries along both the eastern and western shore, surviving numerous stresses and are of considerable historical, cultural and ecological importance (Terral et al. 2004). The olive tree still remains a key component of agriculture today and will be into the future. Therefore, genetic characterization of olive varieties and genetic resources (Khadari et al., 2019; Galatali et al., 2021), description based

on morphological characters and phenology of growth stages of olive trees (Sanz-Cortés et al., 2002), experimentation through field irrigation and/or more rarely through drought stress treatments (Alcaras et al., 2016) have been conducted to avoid genetic erosion, optimize the water use for irrigation and hence improve orchard management, and solely to better understand the biodiversity. Only few studies have focused on the response of the olive tree to Hg pollution in its natural Mediterranean environment (Higueras et al., 2012; Higueras et al., 2016; Guarino et al., 2021; Labdaoui et al., 2021).

Lebanon, a small country at the Eastern Mediterranean, is facing important anthropogenic pressure within a changing environment (Gérard and Nehmé 2020). The air quality in Lebanon all over the country is noted to be moderately unsafe with an annual mean concentration of 31 $\mu g/m^3$ of PM2.5 (Particulate Matter) which is above the maximum recommended value (10 $\mu g/m^3$) (Lebanon: Air Pollution IAMAT 2020). Adding to that, soil samples collected from different areas in southern Lebanon showed values of Hg concentration ranging between 160-6480 ng/g showing a high contamination levels (Borjac et al. 2020) as indicated by World reference Senesil et al., 1999; Kabata-Pendias & Pendias, 2000. The main contributors of the air pollution include cement industries, mineral and chemical factories, vehicles emissions, food processing and oil refining. Ancient olive groves are found across different agroclimatic areas at different altitudinal belts, still producing olives and oil for consumption with these various pollution pressures. In this study two sites, known for their century-old olive groves and located at two different altitudes in Lebanon, were selected to assess the Hg contents. In these remote areas, no direct sources of mercury contamination are reported and hence we expect very low Hg concentrations. However, due to atmospheric transport of Hg, dry or wet deposition of Hgcan be expected in remote areas (Grigal, 2003). The main objectives of this study are to examine and compare Hg levels in foliage, stems, fruits, litter and soil measured in each of these two olive groves, which we monitored monthly for 18 months. The second objective is to analyze the relative importance of Hg uptake by the soil and foliage in comparison with the atmospheric Hg. Since the distribution of Hg pollution is by nature geographically widespread, and given the extent of Hg pollution in the Mediterranean and the transfer of pollution by wind and the Mediterranean Sea, long-distance contamination occurs over large areas. This study may draw an adequate baseline for Eastern Mediterranean and region of similar climates inventories on Hg vegetation uptake and new studies on olive trees in the Mediterranean to reconstruct regional Hg pollution concentrations in the past and present.

2. Materials and methods

Two monumental olive groves were chosen in the context of their historical and agricultural importance, since these two sites are considered to contain olive trees more than 1400 years old and are still productive.

2.1. Geographic setting and environmental context

2.1.1. Bchaaleh site - North Lebanon

This grove is situated in Batroun district (Latitude 34°12’06’’ N, Longitude 35º49’23’’ E, Altitude 1300 m.a.s.l.) (Figure 1). Olive trees are growing rainfed in a sandy loam texture soil of grain size analysis of sand, silt and clay percentages are 52.8 %, 38.7 % and 10.7 % respectively. Soil pH is 7.07 ± 0.26 with organic matter and calcium

carbonate contents are 1.7 % and 38.3 % respectively (Yazbeck et al. 2018). In this study, soil profiles of carbon and nitrogen contents were analyzed. Organic carbon contents decreased with soil depth from about 4 % at 0-1 cm (Soil surface) to 2.7 % at 30-60 cm. The total nitrogen is about 0.3 % at 1cm depth and 0.2 % at 30-60 cm depth. The olive trees are located on two terraces. The first terrace is at 1.5 meter above the road level while the second is at the road level. They are maintained by the municipality for the last four decades as an endowment property. Precipitation average ranges between 229 and 392 mm in winter and between zero and less than 2 mm/season in summer, while average temperature is between 4 and 8 °C in winter and between 20 and 23 °C in summer and average relative humidity of 63% (data extracted from LARI climatic data) (Table S1, Figure S1).

The village is at about 36 km from Chekka town located at a lower altitude (0-200 m.a.s.l.) nearby the sea (Figure 1), and which is classified as a source of air pollution (EJOLT 2019)**.** Chekka is the site of an important national cement factory responsible of carbon dioxide, sulfur dioxide, nitrous oxides, carbon monoxide and particulate material emissions causing respiratory and health issues (Kobrossi et al. 2002) and water pollution (Nassif et al. 2016). At 28 km from Bchaaleh, the small commercial port of Selaata (0-37 m.a.s.l.) emits many pollutants (ie. Phosphogypssum, heavy metals, radionuclides) expanding via water and air pathways (Petrlik et al. 2013; Yammine et al. 2010). To our knowledge no direct Hg pollution is reported at Chekka and Selaata sites. However a dissolved gaseous Hg from natural and human activities is saturated in the upper Eastern Mediterranean Sea, Gårdfeldt et al., (2003) have evidenced that Mediterranean Sea is a source of airborne elemental Hg.

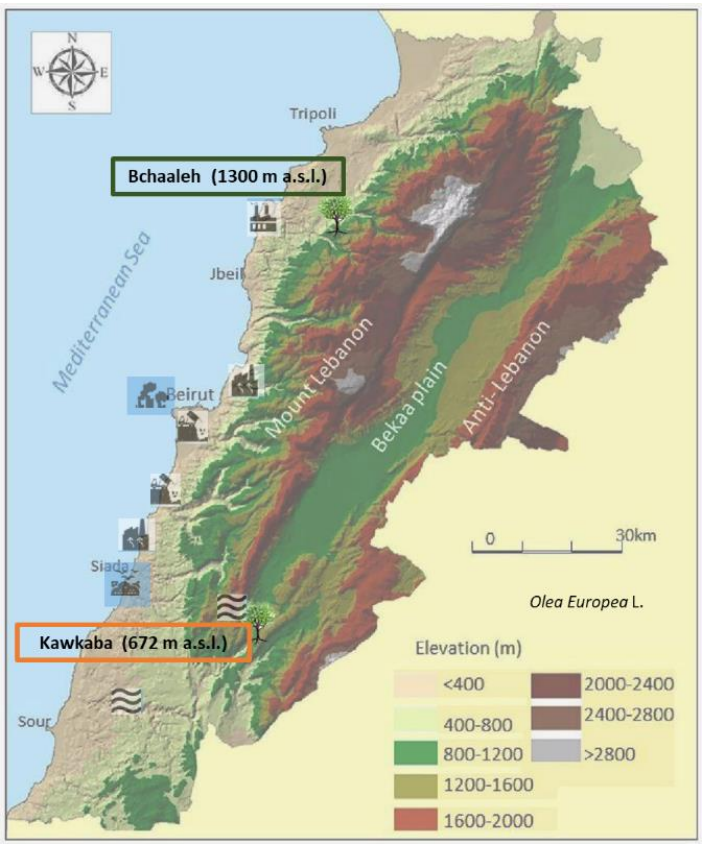

Figure 1. Site locations of the two selected focus areas (modified after Shared Water Resources of Lebanon, Nova Science Publishers 2017).

2.1.2. Kawkaba site - South Lebanon

The second grove is located in the village of Kawkaba, South Lebanon (Latitude 33°23'856'' N, Longitude 35°38'588'' E, Altitude 672 m.a.s.l. (Figure 1). Kawkaba soil is characterized as clay loam soil of pH 7.5 ± 0.5. Soil organic material and calcium carbonate average are 1.7 % and 59.0 % respectively (Al-Zubaidi et al., 2008) and grain size analysis of sand, silt and clay percentages are 6 %, 28 % and 66 % respectively. The analysis of organic carbon and nitrogen at the 0-1 cm and at 0-30 cm decrease from about 9.0 % to 2.2 % and from 0.9 % to 0.3 % for the carbon and nitrogen respectively. Average precipitation ranges between 215 and 374 mm in winter and drop to almost zero mm in summer, while average temperature is between 7 and 11 °C in winter and between 21 and 27 °C in summer and relative humidity of 61% (data extracted from LARI climatic data) (Table S1, Figure S1).

The village has to its east the Hasbani river, originated from the north-western slopes of Mount Hermon in Hasbaya (36 km away from Kawkaba and located at 750 m.a.s.l.) (Badr et al. 2014; Jurdi et al. 2002). On the other hand, the Litani River (170 km long and located at 800 to 1000 m.a.s.l) (Figure 1) rising in the south of the Bekaa valley is about 29 km away from Kawkaba (Abou Habib et al. 2015, Khatib et al. 2018). These two rivers are polluted and for these reasons they are not used for irrigating crops in Kawkaba and surrounding areas while the olive trees are growing rainfed as per indicated by the municipality of Kawkaba. Here as well, we did not find indication of direct Hg pollution. Climatic data in both Bchaaleh and Kawkaba were collected from meteorological station and manual rain gauge installed in the villages by LARI (Lebanese Agricultural Research Institute). CO_2 data used in this study are from NOAA Global Monitoring Laboratory (https://gml.noaa.gov/webdata/ccgg/trends/co2/co2_trend_gl.txt).

2.2. Field sampling

For the Hg concentration analysis, four olive trees ~~of 8 to 15 m foot circumference~~ (3-5 m in diameter and an average height of 4-6 m) were sampled in each of the two groves from February 2019 to September 2020. Within Bchaaleh two trees were selected from the upper terrace (BCO1-Bchaaleh-Tree 1, BCO4-Bchaaleh-Tree 4) and two other trees were sampled from a lower terrace located 1.5 m below the upper one (BCO9-Bchaaleh-Tree 9, BCO12-Bchaaleh-Tree 12) (Figure S2). In Kawkaba, four trees were selected and sampled (KWO1-Kawkaba-Tree 1, KWO2-Kawkaba-Tree 2, KWO3-Kawkaba- Tree 3, KWO4-Kawkaba-Tree 4). For each olive tree, both sun exposed and shaded foliage and stems (terminal portions of 20 cm) with no evidence of pathogens were randomly taken and merged from the upper, middle, and lower canopy position of the olive trees on a monthly basis using a manual pruner. The phenological growth stages of olive trees described by Sanz-Cortés et al.,(2002) in Spain suggest leaf development from March to November. Hence it should be mentioned that the Hg concentration measured on monthly collected foliage represents an average of Hg accumulated in young foliage (year N of collection where N is equal to 2019 and 2020) and older foliage (N-1 year and N-2 years). Fruits were collected in April 2019. Litter and soil surface were separately collected on the whole top surface area of the olive groves and stored in different paper bags once every four months. In parallel, soil sampling was performed using a bucket auger to a maximum depth of 60 cm. In both

sites Bchaaleh and Kawkaba, the soil showed uniform color and texture. Soil cores were fractioned in soil surface (0-1 cm), 0 to 30 cm depth and from 30 to 60 cm depth in order to study the effect and accumulation of Hg concentration on the different depth layers. To avoid contamination, gloves were worn while collecting samples, and the equipment was rinsed with methanol between every sample. A set of 453 samples were collected and stored in paper bags until further preparation for the Hg analysis.

2.3. Sample preparation for Hg analysis

Collected foliage and stems were rinsed with distilled water and then dried for 48 hours in an oven at a temperature of 50°C at maximum (Demers et al., 2013; Li et al., 2017; Pleijel et al., 2021). This procedure likely eliminate any Hg(0) present in the samples. The dried foliage, stems, litter and olive fruits samples were grinded using an electrical stainless grinding machine with no heating system for 5-10 minutes, while soil samples were prepared with a manual natural agate grinder. All samples were later sieved using an inox stainless-steel 125-micron sieve mesh to collect homogeneous powders for analysis. A total of 150 mg for foliage and soil (50 mg/analysis), and 300 mg of litter and stems (100 mg/analysis) were considered in triplicates for analysis of Hg concentrations.

2.4. Analytical method

For the Hg elemental analysis, a total of 453 powder samples from foliage, stem, grain, litter and soil were analyzed using an advanced Hg analyzer AMA 254 (Altec) as described elsewhere (Barre et al. 2018; Duval et al. 2020). A known amount of sample (50-100 mg) is weight in a nickel boat, using a 10^{-6} g precision balance. The sample aliquot is first dried at 120°C for 60s and subsequently pyrolyzed at 750°C for 150s, under oxygen flow. The resulting gaseous Hg produced during the sample decomposition is amalgamated on a gold trap and then released to an Atomic Absorption spectrometer after a thermal desorption step at 950°C. The AMA 254 instrument was calibrated through several external matrix-matched calibration procedures using the following certified reference materials: IAEA-456 sediment (77 ± 5 ng Hg/g), NIST-1575A pine needles (39,9 ± 0,7 ng Hg/g) and IAEA336 (200 ± 40 ng Hg/g). The QA/QC evaluation of the analytical procedure was completed with a continuous monitoring of the blank's values (Nickel boat Hg background noise), every 15 analyzed samples. The precision of the measurements was assessed through replicated analyses (n=2) of 13 % of the total amount of samples (n=453). Average relative standard deviations of 5 % and 2.5 % are thus associated to the reported Hg concentrations for the 2019 and 2020 samples batches, respectively. The absolute detection limit (ADL) of the analytical technique (AMA 254) was estimated at 0.04 ng Hg. As a consequence, the method detection limit (MDL) for samples analyzed were 0.7 ng Hg/g for soil, litter and foliage and 0.4 ng Hg/g for stem and wood. These MDL were much lower than the measured Hg concentration in the various samples.

Susbamples of soil were used for carbon and nitrogen elemental contents (%) analysis. A 2 mg (acid washed soil and bulk soil) of powders were weighed into tin capsules and measured by dry combustion using a Pyrocube Elemental Analyser (EA, Elementar GmbH).

2.5. Statistical analysis

For the statistical analysis we used the R 4.1.0 program. Our data are not normally distributed, so for the effect of tissue type on Hg concentration, Wilcoxon test was used with the tissue type (foliage and stems) as the main effect. Pearson correlation analysis was used to examine the inter-individual correlation of Hg concentration between the trees. Correlation between Hg concentration of soil surface, litter and foliage was studied using a correlation test. For the seasonal effect (Winter: Mid December till Mid-March, Spring: Mid-March till Mid-June, Summer: Mid-June till Mid-September, Autumn: Mid-September till Mid-December) on Hg concentration, Wilcoxon test was used considering the unequal data available for the different seasons. Finally, the effect of climatic factors (Temperature, precipitation, pCO_2) on Hg accumulation was examined using a Wilcoxon test.

3. Results

3.1. Hg concentrations in plant tissues, litter and soil at Bchaaleh and Kawkaba groves

Hg concentrations measured in the different sampled materials (plant tissues, litter and soil) varied generally according to both tree tissues and groves agroclimatic conditions (Table 1). Hg values in the foliage varied significantly between the two groves (p-value=$1.581*10^{-6}$), where the highest concentration was recorded in Bchaaleh (48.1 ± 10.6 ng/g) *vs.* (35 ± 12.4 ng/g) in Kawkaba. Soil surface also recorded a difference in Hg concentration between Bchaaleh and Kawkaba, with 61.9 ± 20.0 ng/g in Bchaaleh and 128.5 ± 9.4 ng/g in Kawkaba. Soil 0-30 cm samples taken from Bchaaleh and Kawkaba groves, values ranged between 31.8 ± 4.7 ng/g and 70.2 ± 23.4 ng/g respectively. In soil 30-60 cm Hg concentrations recorded 19.5 ± 6.73 ng/g at Bchaaleh. No significant differences were recorded for litter and stems Hg concentrations (p-value= 0.0915 and p-value=0.2215 respectively) between the groves, with litter values of 62.9 ± 17.8 at Bchaaleh and 75.7 ± 20.3 ng/g at Kawkaba *vs.* stem values of 7.9 ± 2.8 ng/g at Bchaaleh and 9.0 ± 4.7 ng/g at Kawkaba. Positive correlations were observed between soil and litter in Bchaaleh (r=0.60) and Kawkaba (r=0.95) though statistically insignificant (p-value= 0.40 and 0.13 respectively).

The comparison between Bchaaleh and Kawkaba soil surface Hg contents showed significant difference between the two groves (p-value=0.04746). We observe the same significant difference when comparing the soil horizon of 0-30 cm of both groves. In descending order of Hg concentrations and considering the different sites, plant tissue, soil and litter samples, the Hg concentrations could be ranked in Bchaaleh, soil surface > litter> foliage > soil 0-30 cm > soil 30-60 cm > stems > fruits; and in Kawkaba, soil surface > litter > soil 0-30 > foliage > soil 30-60 > stems > fruits (Table 1).

Table 1. Overall mean values of Hg concentration (ng/g) of the different studied material in both Bchaaleh and Kawkaba olive groves

Sample material	Bchaaleh (BC)			Kawkaba (KW)		
	Average (ng/g)	SD	N	Average (ng/g)	SD	N
Foliage	**48.1**	**10.6**	**66**	**35.0**	**12.4**	**67**
Stems	**7.9**	**2.8**	**66**	**9.0**	**4.7**	**67**
Litter	**62.9**	**17.8**	**7**	**75.7**	**20.3**	**6**
Soil Surface	**61.9**	**20.0**	**8**	**128. 5**	**9.4**	**6**
Soil 0-30cm	**31.8**	**4.7**	**6**	**70.2**	**23.4**	**5**
Soil 30-60cm	**19.5**	**6.7**	**5**	**28.0**		**1**
Fruits	**7.0**	**3.5**	**3**	**11.0**		**1**

3.2. Seasonal variation of Hg concentration in plant tissues, litter and soil

Hg concentrations recorded between February 2019 and September 2020 (Table 2) reflected a significant seasonal variation in both sites (p-value<$2.2*10^{-16}$)

In Bchaaleh grove, foliage registered its highest Hg concentration during winter and spring with 61.8 ± 7.6 ng/g and 55.1 ± 12.5 ng/g respectively, and its lowest Hg amount during summer and autumn with 41.5±12.7 ng/g and 44.4 ± 6.2 ng/g, respectively. A seasonal effect on foliage and stems was registered (p-value<$2.2*10^{-16}$; Figure 2a,c). The stems and soil 0-30cm highest values was registered in autumn. Significant differences were found in foliage Hg values between summer and winter (p-value=0.00020), and autumn and winter (p-value= 0.00014). Similarly, stems Hg values varied significantly between spring and winter (p-value=0.030), autumn and winter (p-value=0.047). Litter highest Hg content occur in summer in Bchaaleh olive groves (79.3 ± 26.5 ng/g) and the lowest in winter (48.6 ± 13.3 ng/g) (p-value = 0.2286). Highest Hg contents in the soil surface of Bchaaleh is recorded in summer (84.5 ± 21.2 ng/g).

In Kawkaba, the highest Hg concentrations for foliage and stems were registered in spring with 51.8 ± 4.5 ng/g, 11.7 ± 6.7 ng/g respectively (Table 2, Figure 2b,d). Significant differences were found in foliage Hg values between summer and winter (p-value=0.013), autumn and winter (p-value= 0.00067), autumn and spring (p-value=$1.589*10^{-05}$), spring and winter (p-value= $9.383*10^{-05}$) and spring and summer (p-value=$2.327*10^{-06}$). Similarly, stem Hg values varied significantly between spring and winter (p-value=0.006), spring and summer (p-value=0.0036) and autumn and spring (p-value=0.011). There is no seasonal variation between the litter different seasons for Bchaaleh nor for Kawkaba. Bchaaleh and Kawkaba groves soil surface, 0-30 cm and 30-60cm Hg values varied significantly between seasons, (p-value < 0.05). A seasonal variation is observed in both olive groves especially in the foliage.

Table 2. Seasonal mean Hg concentration (ng/g) and standard deviations of the different studied material in both Bchaaleh and Kawkaba olive groves. Grey color indicated the highest Hg concentration values among the different elements during the different seasons

Hg (ng/g)												
Bchaaleh	**Spring**	**SD**	**N**	**Summer**	**SD**	**N**	**Autumn**	**SD**	**N**	**Winter**	**SD**	**N**
Foliage	55.1	12.5	16	41.5	12.7	24	44.4	6.2	12	61.8	7.6	18
Stems	7.8	3.8	16	7.61	3.9	24	8.3	2.7	12	6.4	2.9	18
Litter	79.3	26.5	3	64.7	4	4	55.5	3.54	2	48.6	13.3	3
Soil Surface	58.3	13	3	84.5	21.2	4	50		1	50.6	23.5	3
0-30cm	33.6	6.2	2	32.2	4.3	2	34.5	7.79	2	27	0.7	3
30-60cm	23.1	9.1	2	20.7	10.32	2	19.6	9.05	2	11		1
Kawkaba	**Spring**	**SD**	**N**	**Summer**	**SD**	**N**	**Autumn**	**SD**	**N**	**Winter**	**SD**	**N**
Foliage	51.8	4.5	16	28	7.2	24	28.5	7.2	16	33.9	5.6	18
Stems	11.7	6.7	16	6.5	1.4	24	7.7	2.1	16	6.9	1.6	18
Litter	90.1	29.3	2	67	24	2	70	1.4	2			
Soil Surface	132	8.5	2	118	4.2	2	135.6	2.2	2			
0-30cm	57.9	11.2	2	65.8		1	84.8	36.4	2			
30-60cm	28		1									

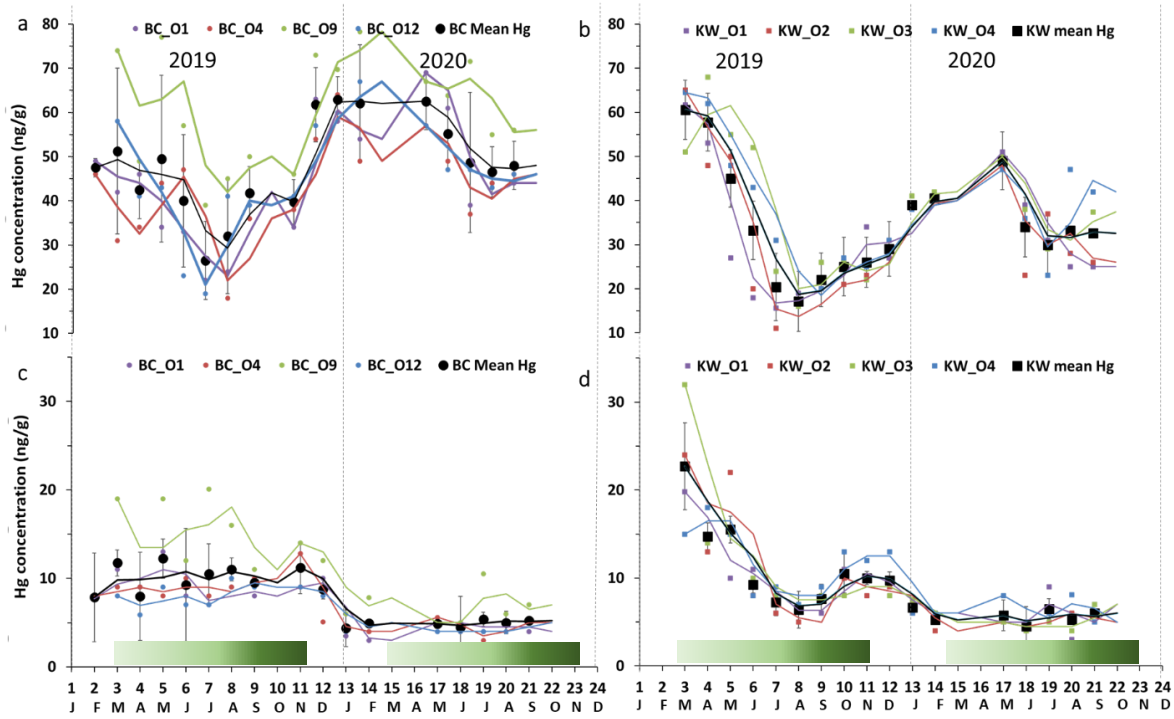

Figure 2. Seasonal variations of foliage Hg concentration in(**a)** Bchaaleh (BC) and (**b)** Kawkaba (KW) olive groves and stems Hg concentration in **(c)** Bchaaleh and **(d)** Kawkaba olive groves. Shaded green horizontal bars represent the leaf development of olive trees during the growing season of cultivars in Spain according to the BBCH scale (Sanz-Cortès et al., 2002).

3.3. Inter-individual variability between trees for each site

In the upper terrace of Bchaaleh grove, the foliage average Hg concentration of BCO4 and BCO1 varied between 42.4 ± 11.5 ng/g and 44.6 ± 13.3 ng/g respectively showing no significant difference (p-value = 0.8225). In the lower terrace of the same site, foliage average Hg concentrations of trees BCO12 and BCO9 were found to vary from 45.6 ± 12.7 ng/g to 60.7 ± 12.7 ng/g respectively (Figure 2a) exhibiting a significant difference ((p-value=0.0059). Tree BCO9 is significantly different to each of the three trees (p-value< 0.0059) while BCO1, BCO4 and BCO12 have very similar Hg contents (p-value= 0.46).

In the upper terrace of Bchaaleh grove, the stems average Hg concentration of BCO4 and BCO1 varied between 7.0 ± 2.8 ng/g and 7.1 ± 2.9 ng/g respectively showing no significant difference (p-value= 0.94). In the lower terrace, stems average Hg concentrations of BCO12 and BCO9 are 6.4 ± 2.2 ng/g and 11.2 ± 5.2 ng/g respectively showing a significant difference (p-value= 0.0054; Figure 2c). For BCO1 and BCO12 there was no significance difference (p-value= 0.5725), the same goes for BCO4 and BCO12 (p-value= 0.523).

The average concentration per tree in foliage and stems were 32.4 ± 12.2 ng/g and 8.5 ± 4.0 ng/g respectively for KWO1, 32. 8 ± 14.7 ng/g and 8.9 ± 6.0 ng/g for KWO2, 37.6 ± 14.0 ng/g and 9.3 ± 6.7 ng/g for KWO3 and 37.7 ± 13.6 ng/g and 9.6 ± 4.0 ng/g for KWO4 (Figure 2b,d). In Kawkaba grove, comparison of the foliage Hg concentration between the four studied trees shows no significant difference (0.22<p-value<1), neither for the stems (0.21<p-value<0.96).

3.4. Hg concentration and agro-climatic effect

At first glance, seasonal variations of the Hg concentrations of the foliage of both sites suggest a covariation with climatic parameters (Precipitation amounts, Relative Humidity and Temperature) (Figure SI) and atmospheric pCO_2. Foliage Hg content increased with higher precipitation and lower temperature (Autumn and Winter) while during the warmer and dryer seasons (May to mid-October), the Hg concentration of foliage decreased (Figure SI). However, the Wilcoxon test for a non-normal distribution shows no significant correlation between Hg concentration of foliage and precipitation (p-value= 0.95). While temperature, relative humidity and atmospheric CO_2 (pCO_2) shows a significant correlation (p-value = $2.2e^{-16}$). For the stems, Hg concentration also showed no significant correlation with precipitation (p-value= 0.1147), and a significant correlation with temperature, relative humidity and pCO_2 (p-value= $2.2e^{-16}$).

4. Discussion

4.1. Hg concentration in plant tissues, soil and litter in the studied groves

In both groves our values showed a higher Hg concentration in the olive foliage (Bchaaleh average of 48.1 ± 10.6 ng/g; Kawkaba average of 35.0 ± 12.4 ng/g), than that of the stems (Bchaaleh average of 7.9 ± 2.8 ng/g; Kawkaba average of 9.0 ± 4.7 ng/g) and that of olive fruits (7 ± 3.5 ng/g at Bchaaleh, n=3 and 11 ng/g in Kawkaba, n=1). Our data corroborates previous studies (Bargagli 1995; Higueras et al. 2016) showing that olive foliage has the highest Hg

concentration of plant tissues. Our values are lower than 200 ng/g considered as Hg pollution threshold (Kabata-Pendias & Pendias, 2000) and implying no pollution effect for both Bchaaleh and Kawkaba groves (Table S2; Figure S3a,b). This suggests that our sites are good remote bioindicators of the uptake of Hg through the plant, although more prolonged time range study is needed. However, in an overview of vegetation uptake of mercury and impacts on global cycling, Zhou et al., (2021) suggested lower values for unpolluted sites (litterfall 43 ng/g > foliage 20 ng/g and branch 12 ng/g). Knowing that our sites correspond to unpolluted areas of Lebanon, the lower values of Zhou et al., (2021) obtained from an ensemble of various species (trees and grasses) and not specifically on olive trees, we considered that the threshold value of 200 ng/g (Kabata-Pendias and Pendias 2000) is more adapted to our comparison.

As described in several studies, Hg in foliage originates predominantly from the atmospheric gaseous Hg(0) through stomatal uptake (Ericksen et al., 2003; Lindberg et al., 1979; Zhou et al., 2021). Adding to that, the atmospheric Hg uptake in foliage excedes Hg stomatal re-emission (Pleijel et al., 2021; Zhou et al., 2021). Inside the leaves the oxidized Hg(II) has high affinities to bind covalently with organic groups (Du & Fang, 1983; Clarkson & Magos, 2006; Pleijel et al., 2021). The Hg can be translocated by phloem transport to the stems and eventually into roots and potential release into soils may also be contributing to Hg accumulation in soils (Giesler et al., 2017; Schaefer et al., 2020).

The soil surface and litter registered the highest Hg concentration (62 to 129 ng/g) among all samples (foliage, stems, fruit) in both groves (Table 1) suggesting that the soil is the main Hg reservoir through the Hg throughfall and litter inputs (Tomiyasu et al., 2005). Our findings are in agreement with studies on evergreen forest ecosystems reporting that soil can hold more than 60 % of Hg input to the forest floor (Wang et al. 2016). Our soil surface sites values (61.9 ± 20.0 ng/g in Bchaaleh and 128.5 ± 9.4 ng/g in Kawkaba) show higher Hg concentration in Kawkaba compared to the general background level of Hg as defined by uncontaminated soil world reference mean Hg contents (20 to 100 ng/g; Kabata-Pendias and Pendias 2000; Senesil et al. 1999; Gworek et al. 2020). However, both sites have significantly lower values compared to known industrial and mining contaminated sites (> 1000 ng/g ;). Nevertheless, studies conducted in different sites show a wide range of natural background Hg levels (ie. topsoils in Europe, India, Brazil, Norwegian Arctic, New Zealand have values of 40, 50, 80, 110, 230 ng/g respectively) (Gworek et al. 2020) making it difficult to set a specific Hg threshold value for uncontaminated soil (Table S2; Figure S3c). Due to the differences registered in different countries and sites of sampled soil, this indicates a link with chemical and mineralogical soil properties (ie. pH, humic acid, soil grain size distribution, organic matter type and clay percentage) affecting Hg in soil and its transport (Richardson et al., 2013; Chen et al., 2016; O'Connor et al., 2019). Nitrogen can also be a factor affecting the Hg content in soil depending on its characteristics. Nitrogen increase can change the equilibrium of soil solution and the morphology of roots, causing a possible increase in Hg availability in soil and increases the Hg uptake by the plant (Alloway, 1995; Barber, 1995; Carrasco-Gil et al., 2012). The increase in Hg availability in the soil is due to the organic Nitrogen that provides a high absorption capacity, retaining the atmospheric Hg deposition (Obrist et al., 2009). Nitrogen supply prevents oxidative stress in roots, but also can improve root development and increase the uptake of Hg from the soil (Carrasco-Gil et al. 2012). Hence, we suggest that lower values in Bchaaleh soils are likely explained by the low clay, organic carbon and nitrogen contents (10.7 %, 4 % and 0.3 % in soil surface respectively).While Kawkaba higher Hg soil contents can be explained by the higher clay

proportion (66 %) and organic carbon and nitrogen contents (9 % and 0.92 %). On such clay loam soils and rich organic matter, Hg binding is facilitated explaining higher content (O'Connor et al. 2019).

The litter showed higher Hg concentration than that in foliage in both Bchaaleh (62.9 ± 17.8 ng/g) and Kawkaba (75.7 ± 20.3 ng/g) (Table 1). This has been also described by Rea et al., (1996) and Zhou et al., (2021) in uncontaminated and contaminated sites where litterfall Hg contents were systematically higher than the foliage Hg contents. The bacterial and chemical decomposition of the litter decrease significantly the amount of C compared to the Hg that conversely may continue to increase due to the continued absorption of Hg from precipitation and throughfall (Obrist et al., 2011; Pokharel & Obrist, 2011; Zhou et al., 2021). Another possible explanation is that the leaves shed as litter are likely to mostly be the oldest leaves which have accumulated Hg during the longest period of time and thus have higher Hg concentrations than the remaining foliage have on average since they consist of both younger and older foliage (Rea et al. 1996; Pleijel et al. 2021).

4.2. Seasonal foliage Hg content versus seasonal atmospheric Hg and CO_2

The late winter-early spring registered the highest Hg concentration for foliage in both groves, while summer and early fall to a less extent recorded the lowest concentrations. This seasonal change is explained by the seasonal tree physiology variations such as the Hg accumulation in leaves after stomatal uptake (Pleijel et al., 2021; Wohlgemuth et al., 2021). We can suggest that during winter-early spring, water is available and photosynthetic activity is not limited, hence both CO_2 and Hg diffuse through opened stomata inside the foliage. As shown on figure 2, Hg in foliage is low in summer-fall and hence act as a sink of Hg. Note that despite we mixed three generations of olive leaves (year N to N-3), the most recent of which are known to be low in mercury (Pleijel et al., 2021), the seasonal signal is still very remarkable. Therefore, one can speculate that the mercury levels would have been higher if we had avoided the recently formed foliage during spring and early summer. This may also explain the large difference in Hg levels between litter and foliage.

At our latitudes, Bchaaleh and Kawkaba foliage evergreen olive trees show a decrease in Hg contents from end of March to late August, with minimum values centered in August suggesting a decline of the plant Hg uptake likely explained by the reduction of the stomatal conductance (Lindberg et al., 2007; Pleijel et al., 2021). This minimal photosynthetic activity occurs during the driest season (0 mm precipitation) and hottest temperatures (above 25°C) at our sites. Year 2020 has higher foliage Hg values than 2019. This can be related to a higher vegetation uptake in 2020 in comparison to 2019. Martino et al., (2022) showed seasonal variability of Gaseous Elemental Mercury (GEM) in the atmosphere in southern Italy (Figure 3a). They also related this seasonality to high energy use for heat during winter thus higher emissions due to coal combustion (Weigelt et al., 2015) and the effect of air mass trajectory on the GEM seasonality where the winter peak is connected to the Hg re-emission from sea surface and with long-range transport, in addition to the GEM oxidation rate in warmer months (Horowitz et al., 2017; Martino et al., 2022). Martino et al. (2022) comparing the normalized difference vegetation index values (NDVI) with GEM concentration of the same seasons over the different years (2018 to 2020), show that the higher vegetation uptake explains the GEM depletion in certain seasons and years. This was also collaborating Jiskra et al., (2018) for the Northern Hemisphere site. Since no data of atmospheric mercury in Lebanon or surrounding countries are available we used the atmospheric

Hg time series data of Martino et al. (2022) (Figure 3a). We observed opposite trends between foliage Hg concentration and air Hg (negative covariation in 2019 and positve covariation in 2020) (Figure a,d,e).

Alternatively other studies reported a positive correlation between atmospheric Hg and crops (Niu et al. 2011) as observed in our study between the $Hg_{foliage}$ and the atmospheric Hg in 2020 (Figure 3a,d,e). This suggest the hypothesis where our groves seasonally exposed to high atmospheric Hg, accumulate Hg in their foliage (Lindberg et al. 2007; Pleijel et al. 2021). According to Hanson et al. (1995), a compensation point for Hg uptake by plant foliage can be considered but no information to our knowledge is available for the specific case of the olive trees. The tight link between foliage Hg uptake and stomatal conductance seasonal variations can be also deduced from the analysis of the partial pressure of the pCO_{2atm} seasonal variation (Obrist, 2007; Jiskra et al., 2018; Obrist et al., 2018; Pleijel et al., 2021) (Figure 3b,d,e). Very good covariation between olive foliage Hg and pCO_{2atm} are shown for Bchaaleh and Kawkaba despite a notable offset of one month at Kawkaba to two months at Bchaaleh can be deduced (Figure S4). Taking into account our calculated time lags, we obtained significant correlations between our foliage Hg content and pCO_{2atm} of 0.718 and 0.704 in Bchaaleh and Kawkaba respectively. Interestingly a one month time-lag between atmospheric Hg and pCO_{2atm} is also reported by Jiskra et al. (2018) for most northern hemisphere sites. The offset of one to two months between maxima of Bchaaleh and Kawkaba foliage Hg (March/April) and pCO_{2atm} (May) suggests that the minimum of Hg in the foliage occur during the decreasing phase of the pCO_{2atm} when the global northern hemisphere tend to become a net sink of CO_2. When minimum values of pCO_{2atm} are reached at the end of the dry summer (Figure 3b), concomitant to minimum atmospheric Hg (Figure 3a), end of the drought and increase of precipitation (Figure 3c), Bchaleh and Kawkaba olive trees show a recovery in the Hg uptake rates. The photosynthetic activity and the stomatal conductance related to the climatic parameters (temperature, precipitation, humidity, pCO_2) as shown by Ozturk et al. (2021) and the atmospheric Hg explain our foliage Hg seasonal cycle. At a regional scale, our sites show different time lags between Bchaaleh and Kawkaba that we cannot explain fully except their altitudinal differences, which can suggest that Bchaaleh grove benefits of less drought in summer. This can also be explained by the physiology of olive trees that is characterised by small foliage surface area as a response to the high temperature and less humidity in summer and the stomatal conductance in the foliage that increase in winter and decrease in summer. As per Connor & Fereres, 2010, the olive tree is a day neutral plant were its reproductivity is affected by temperature and sunlight. Its vegetative growth is limited by the low temperature in the winter season and water supply in the summer season. The water loss from the foliage due to transpiration and temperature, creates a replacement for water source to be the soil through the roots. The xylem being the main transporter between the roots and the canopy. During the day the evaporation increase and the plant water content decreases and become minimal during midday, noting that the soil water content is high. During the evening the olive tree seeks soil water as an equilibrium. If soil water is not available enough to cover the olive need, the evergreen olive is able to adapt through conservation of internal water especially during severe summer drought, due to its ability to restrict water loss to the atmosphere and maximize extraction of soil water (Connor & Fereres, 2010). Taking into account Hg results obtained during several seasonal campaigns in the surface waters of the Mediterranean Sea and the above atmospheric layer, it has been evidenced that the highest Hg fluxes to the atmosphere occur mainly in summer (Wangberg et al. 2001; Kotnik et al. 2014). Moreover, a higher total gaseous mercury (TGM) is registered in the eastern Mediterranean compared with the

western Mediterranean and Northern Europe (Wängberg et al., 2001). Olive trees are known to be a mycotrophic plant. Mycorrhiza acts as a barrier that restrict the movement of heavy metals from the roots to the plants (Wu et al., 2016; Riaz et al., 2021). In the Mediterranean region, it is reported that intensity of mycorrhizal colonization of olive tree roots increases with the increase of seasonal precipitation/decrease in temperature and decreased with the increase of air temperature, when it is drier (Meddad-Hamza et al., 2017). This confirms that in the decrease of mycorrhizal activity in summer, a possible minimal Hg uptake from the soil and roots to the foliage and stems through water during the drought season may occur (Rea et al., 2002; Meddad-Hamza et al., 2017). Further analysis and data are necessary to confirm the above assumption.

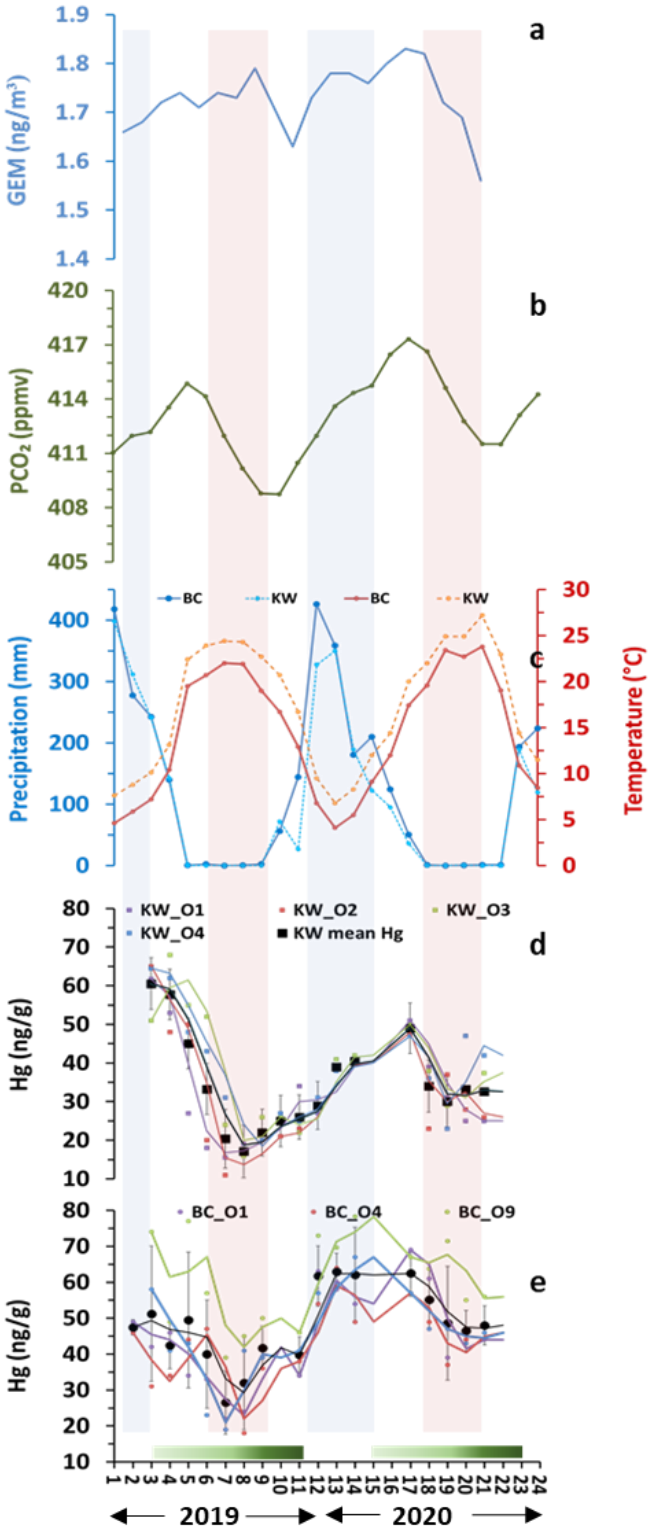

Figure 3. Seasonal variations of (**a)** atmospheric Hg(0) (Martino et al. 2022), (**b)** pCO_2 (NOAA Global Monitoring Laboratory), (**c)** precipitations and temperature of Bchaaleh and Kawkaba respectively and (**d)** and (**e)** foliage Hg concentration in Bchaaleh and Kawkaba olive groves respectively. Shaded green horizontal bars represent the leaf development of olive trees during the growing season of cultivars in Spain according to the BBCH scale (Sanz-Cortès et al., 2002). Shaded colored lines correspond to the Winter (Blue) and Summer (Red).

4.3. Hg cycling in the stems, litter and soil system

For each site, Hg contents in stems exhibit narrow range between the different trees except tree BCO9, which had the highest stem values. We speculate that this higher Hg content is the adjunction of chemical products as fertilizer on the plot 549 belonging to a different owner (Figure S2) likely between fall and winter. It was observed by (Zhao & Wang, 2010) that the fertilizer used and its source of phosphorous may affect the Hg content in the product and thus affect the amount of Hg transported into the fertilized soil.

At a seasonal scale, the averaged Hg values of soil system show statistical significance differences between the four seasons, while stems show a significant difference between winter (lowest values) and spring (p-value= 0.030) and winter-autumn (p-value= 0.047) in Bchaaleh grove mostly similar to foliage changes. While litter shows no significant difference between seasons. The same behavior was registered in Kawkaba in litter and soils, while stems showing statistical significance differences between autumn and spring (p-value= 0.011), spring-winter (p-value= 0.006) and spring-summer (p-value= 0.004) (Table 2). Despite the small amount of Hg content in the stems, the statistically significant seasonal changes may suggest that small amount of Hg move from the foliage to the lignified tissues as stems. However, we cannot neglect the Hg transport in xylem sap from the roots to the aboveground plant tissues even if minimal (Yang et al. 2018).

We can suggest the following Hg cycling in the system of the olive grove/soil. In winter-early spring the highest concentrations in foliage continuously feed the litter and can explain the following maximal spring Hg content of the litter. The decomposition of the litter organic matter during the wettest conditions likely liberate Hg in the Hg(0) or Hg(II) forms or MeHg either towards the atmosphere or the surface soil (see Table 2) respectively (Gworek et al., 2020). A fraction of the degraded organic matter is transferred through gaseous evaporative processes towards the atmosphere while another fraction of the Hg is leaching towards the deeper soil in addition to dry Hg deposition during dry season (Teixeira et al. 2017). We can also speculate that the small Hg decrease observed in soil 0-30, 30-60 cm during the winter season in Bchaaleh can be due to the minimal absorption of total Hg and MeHg through the roots and xylem sap to the above ground tissues (Johnson and Lindberg 1995).

5. Conclusion

This is the first study conducted on monumental olive trees in a remote site of the MENA region without local contamination and followed at a monthly basis over 18 months. Findings of our study indicate a higher uptake of Hg in the olive foliage compared to stems, fruits items and a remarkable $Hg_{Foliage}$ seasonal variation in both studied groves. Winter and Spring were particularly suitable for Hg accumulation in foliage in both sites. The significant correlation between our $Hg_{Foliage}$ contents and the atmospheric Hg content and pCO_2, despite the one to two months' time lag, suggests that the main source of $Hg_{Foliage}$ is the atmospheric Hg as observed in different species and studies (conifers and hardwood). Hg is absorbed by the foliage, via the open stomata, driven by the interaction of high vegetal activity, temperature, water availability and the processes that control transpiration, which is likely to be seasonal. Hence physiological and climatic processes explain the seasonal Hg accumulation in foliage. Thus, a more intensive study taking account the phenological dynamics of olive tree foliage must be focused on. Further comparison and studies on the seasonal atmospheric Hg in the eastern Mediterranean basin are necessary to test our hypothesis of the reversed

seasonality of Hg in 2019 and positive covariation in 2020 since contrary to the global Northern Hemisphere and western Mediteranean region vegetation, our olive groves act as a sink of Hg and CO_2 when global Northern and western Mediteranean vegetation is emitting. This relationship $Hg_{Foliage} - Hg_{atm}\text{-}pCO_{2atm}$ should be further investigated along the season and locally to better understand the observed time lags. Soil surface registered the highest Hg concentration among all studied compartments due to well-known processes of litter and throughfall that incorporate Hg to the soil surface. Moreover, this study highlights significant differences between Hg_{soil} in Bchaaleh and Kawkaba groves due to differences in soil characteristics. In this study we worked on the present time samples in order to have a better understanding of the Hg cycle in the olive tree. Our main contribution in this study is to see how the present-day olive trees records some elements such as Hg to better understand how the Hg in tree rings could be used for the past accumulation records.

Data availability

The datasets generated during and/or analyzed during the current study are available from the corresponding author on reasonable request.

Author Contributions

The corresponding author **Ilham Bentaleb** is responsible for ensuring that the descriptions are accurate and agreed upon by all authors. Conceptualization and methodology were done and developed by **Ilham Bentaleb** and **Lamis Chalak**. The material collection was performed by **Nagham Tabaja**, **Ilham Bentaleb**, **Lamis Chalak**, **Ihab Jomaa, and Milad Riachy**. Sample storage and preparation in Lebanon organized by **Nagham Tabaja**. Material preparation at ISEM by **Nagham Tabaja**, Data collection and analysis were performed by Nagham Tabaja, **Ilham Bentaleb**, **David Amouroux,** and **Emmanuel Tessier**. The setting of the meteorological stations by **Ihab Jomaa**. Subsamples of soil were analyzed for carbon and nitrogen elemental contents (%) by **François Fourel**. The first draft of the manuscript was written **by Nagham Tabaja**. **Ilham Bentaleb, Lamis Chalak**, **David Amouroux, Ihab Jomaa, and Milad Riachy** commented on previous versions of the manuscript. All authors read and approved the final manuscript. Supervision was done by Ilham Bentaleb and Lamis Chalak.

Competing interests

The authors declare that they have no known competing financial interests or personal relationships that could have appeared to influence the work reported in this paper.

Acknowledgments

The authors would like to acknowledge the National Council for Scientific Research of Lebanon (CNRS-L) and Montpellier University for granting a doctoral fellowship (CNRS-L/UM) to Nagham Tabaja. The authors would also like to thank the Franco-Lebanese Hubert Curien Partnership (PHC-CEDRE) project 44559PL for the funding provided. Institute of Evolutionary Science of Montpellier (ISEM) at Montpellier University and the Research Platform for Environment and Science- Doctoral School of Science and Technology (PRASE-EDST) at the Lebanese University are also acknowledged for their support of the laboratory work. Credits go to the Lebanese Agriculture Research Institute (LARI) for assuring automated weather stations and manual rain gauges per site. The authors are grateful to the Municipality of Bchaaleh (Mr. Rachid Geagea) and the Municipality of Kawkaba (Ms. Mira Khoury). Acknowledgments are extended to Ms. Amira Yousef at LARI for her kind support and to Mr. Akram Tabaja for helping during fieldwork. We are very greatful to Pleijel Hakan who reviewed this article improving significantly our paper. We deeply aknowledgeAndrew Johnston for the English revision.

Funding

This work was supported and funded by Lebanon and Montpellier University (CNRS-L/UM grant), and PHC-CEDRE-project 44559PL

References

References

Abou Habib, N., Taleb, M., & Khoury, R. (2015). *Environmental and social safeguard studies for lake qaraoun pollution prevention project*. *V1*(E4749).

Alcaras, L. M. A., Rousseaux, M. C., & Searles, P. S. (2016). Responses of several soil and plant indicators to post-harvest regulated deficit irrigation in olive trees and their potential for irrigation scheduling. *Agricultural Water Management*, *171*, 10–20. https://doi.org/10.1016/j.agwat.2016.03.006

Alloway, B. J. (1995). *Heavy Metals in Soils*. Springer Science & Business Media.

Al-Zubaidi, A., Yanni, S., & Bashour, I. (2008). Potassium status in some Lebanese soils. *Lebanese Science Journal*, *9*(1), 81–97.

Assad, M. (2017). *Transfert des éléments traces métalliques vers les végétaux: Mécanismes et évaluations des risques dans des environnements exposés à des activités anthropiques*. 218.

Baayoun, A., Itani, W., El Helou, J., Halabi, L., Medlej, S., El Malki, M., Moukhadder, A., Aboujaoude, L. K., Kabakian, V., Mounajed, H., Mokalled, T., Shihadeh, A., Lakkis, I., & Saliba, N. A. (2019). Emission inventory of key sources of air pollution in Lebanon. *Atmospheric Environment*, *215*, 116871. https://doi.org/10.1016/j.atmosenv.2019.116871

Badr, R., Holail, H., & Olama, Z. (2014). *Water quality assessment of hasbani river in south lebanon: microbiological and chemical characteristics and their impact on the ecosystem*. *3*, 16.

Barber, S. A. (1995). *Soil Nutrient Bioavailability: A Mechanistic Approach*. John Wiley & Sons.

Bargagli, R. (1995). The elemental composition of vegetation and the possible incidence of soil contamination of samples. *Science of The Total Environment*, *176*(1–3), 121–128. https://doi.org/10.1016/0048-9697(95)04838-3

Barre, J. P. G., Deletraz, G., Sola-Larrañaga, C., Santamaria, J. M., Bérail, S., Donard, O. F. X., & Amouroux, D. (2018). Multi-element isotopic signature (C, N, Pb, Hg) in epiphytic lichens to discriminate atmospheric contamination as a function of land-use characteristics (Pyrénées-Atlantiques, SW France). *Environmental Pollution*, *243*, 961–971. https://doi.org/10.1016/j.envpol.2018.09.003

Beauford, W., Barber, J., & Barringer, A. R. (1977). Uptake and Distribution of Mercury within Higher Plants. *Physiologia Plantarum*, *39*(4), 261–265. https://doi.org/10.1111/j.1399-3054.1977.tb01880.x

Besnard, G., Khadari, B., Navascues, M., Fernandez-Mazuecos, M., Bakkali, A. E., Arrigo, N., Baali-Cherif, D., de Caraffa, V. B.-B., Santoni, S., Vargas, P., & Savolainen, V. (2013). The complex history of the olive tree: From Late Quaternary diversification of Mediterranean lineages to primary domestication in the northern Levant. *Proceedings of the Royal Society B: Biological Sciences*, *280*(1756), 20122833–20122833.

Bishop, K. H., Lee, Y.-H., Munthe, J., & Dambrine, E. (1998). Xylem sap as a pathway for total mercury and methylmercury transport from soils to tree canopy in the boreal forest. *Biogeochemistry*, *40*, 101–113.

Bishop, K., Shanley, J. B., Riscassi, A., de Wit, H. A., Eklöf, K., Meng, B., Mitchell, C., Osterwalder, S., Schuster, P. F., Webster, J., & Zhu, W. (2020). Recent advances in

624 understanding and measurement of mercury in the environment: Terrestrial Hg cycling.
625 *Science of The Total Environment*, *721*, 137647.
626 https://doi.org/10.1016/j.scitotenv.2020.137647
627 Blackwell, B. D., & Driscoll, C. T. (2015). Using foliar and forest floor mercury concentrations
628 to assess spatial patterns of mercury deposition. *Environmental Pollution*, *202*, 126–134.
629 https://doi.org/10.1016/j.envpol.2015.02.036
630 Boening, D. W. (2000). *Ecological e€ ects, transport, and fate of mercury: A general review*. 17.
631 Borjac, J., El Joumaa, M., Kawach, R., Youssef, L., & Blake, D. A. (2019). Heavy metals and
632 organic compounds contamination in leachates collected from Deir Kanoun Ras El Ain
633 dump and its adjacent canal in South Lebanon. *Heliyon*, *5*(8), e02212.
634 https://doi.org/10.1016/j.heliyon.2019.e02212
635 Borjac, J., El Joumaa, M., Youssef, L., Kawach, R., & Blake, D. A. (2020). Quantitative
636 Analysis of Heavy Metals and Organic Compounds in Soil from Deir Kanoun Ras El Ain
637 Dump, Lebanon. *The Scientific World Journal*, *2020*, 1–10.
638 https://doi.org/10.1155/2020/8151676
639 Briffa, J., Sinagra, E., & Blundell, R. (2020). Heavy metal pollution in the environment and their
640 toxicological effects on humans. *Heliyon*, *6*(9), e04691.
641 https://doi.org/10.1016/j.heliyon.2020.e04691
642 Carrasco-Gil, S., Estebaranz-Yuberob, M., Medel-Cuestab, D., Millán, R., & Hernández, L. E.
643 (2012). Influence of nitrate fertilization on Hg uptake and oxidative stress parameters in
644 alfalfa plants cultivated in a Hg-polluted soil. *Environmental and Experimental Botany*,
645 *75*. https://doi.org/10.1016/j.envexpbot.2011.08.013

Cavallini, A., Natali, L., Durante, M., & Maserti, B. (1999). Mercury uptake, distribution and DNA affinity in durum wheat (Triticum durum Desf.) plants. *Science of The Total Environment*, *243–244*, 119–127. https://doi.org/10.1016/S0048-9697(99)00367-8

Chen, X., Ji, H., Yang, W., Zhu, B., & Ding, H. (2016). Speciation and distribution of mercury in soils around gold mines located upstream of Miyun Reservoir, Beijing, China. *Journal of Geochemical Exploration*, *163*, 1–9. https://doi.org/10.1016/j.gexplo.2016.01.015

Clarkson, T. W., & Magos, L. (2006). The Toxicology of Mercury and Its Chemical Compounds. *Critical Reviews in Toxicology*, *36*(8), 609–662. https://doi.org/10.1080/10408440600845619

Connor, D. J., & Fereres, E. (2010). The Physiology of Adaptation and Yield Expression in Olive. In J. Janick (Ed.), *Horticultural Reviews* (pp. 155–229). John Wiley & Sons, Inc. https://doi.org/10.1002/9780470650882.ch4

Dastoor, A., Angot, H., Bieser, J., Christensen, J. H., Douglas, T. A., Heimbürger-Boavida, L.-E., Jiskra, M., Mason, R. P., McLagan, D. S., Obrist, D., Outridge, P. M., Petrova, M. V., Ryjkov, A., St. Pierre, K. A., Schartup, A. T., Soerensen, A. L., Toyota, K., Travnikov, O., Wilson, S. J., & Zdanowicz, C. (2022). Arctic mercury cycling. *Nature Reviews Earth & Environment*, *3*(4), Article 4. https://doi.org/10.1038/s43017-022-00269-w

Demers, J. D., Blum, J. D., & Zak, D. R. (2013). Mercury isotopes in a forested ecosystem: Implications for air-surface exchange dynamics and the global mercury cycle: Mercury isotopes in a forested ecosystem. *Global Biogeochemical Cycles*, *27*(1), 222–238. https://doi.org/10.1002/gbc.20021

667 Du, S.-H., & Fang, S. C. (1983). Catalase activity of C3 and C4 species and its relationship to
668 mercury vapor uptake. *Environmental and Experimental Botany*, *23*(4), 347–353.
669 https://doi.org/10.1016/0098-8472(83)90009-6
670 Duval, B., Gredilla, A., Fdez-Ortiz de Vallejuelo, S., Tessier, E., Amouroux, D., & de Diego, A.
671 (2020). A simple determination of trace mercury concentrations in natural waters using
672 dispersive Micro-Solid phase extraction preconcentration based on functionalized
673 graphene nanosheets. *Microchemical Journal*, *154*, 104549.
674 https://doi.org/10.1016/j.microc.2019.104549
675 EJOLT. (2019). *Cimenterie Nationale Factory in Chekaa, Lebanon | EJAtlas*. Environmental
676 Justice Atlas. https://ejatlas.org/conflict/chekaa
677 Ericksen, J. A., Gustin, M. S., Schorran, D. E., Johnson, D. W., Lindberg, S. E., & Coleman, J.
678 S. (2003). Accumulation of atmospheric mercury in forest foliage. *Atmospheric*
679 *Environment*, *37*(12), 1613–1622. https://doi.org/10.1016/S1352-2310(03)00008-6
680 Ermolin, M. S., Fedotov, P. S., Malik, N. A., & Karandashev, V. K. (2018). Nanoparticles of
681 volcanic ash as a carrier for toxic elements on the global scale. *Chemosphere*, *200*, 16–
682 22. https://doi.org/10.1016/j.chemosphere.2018.02.089
683 Freeman, M., & Carlson, R. M. (2005). Essential nutrients. *Olive Production Manual*, *3353*, 75.
684 Friedli, H. R., Arellano, A. F., Cinnirella, S., & Pirrone, N. (2009). Initial Estimates of Mercury
685 Emissions to the Atmosphere from Global Biomass Burning. *Environmental Science &*
686 *Technology*, *43*(10), 3507–3513. https://doi.org/10.1021/es802703g
687 Galatali, S., A., N., & Kaya, E. (2021). *Characterization of Olive (Olea Europaea L.) Genetic*
688 *Resources via PCR-Based Molecular Marker Systems*. *2*, 26–33.
689 https://doi.org/10.24018/ejbio.2021.2.1.146

690 Gårdfeldt, K., Sommar, J., Ferrara, R., Ceccarini, C., Lanzillotta, E., Munthe, J., Wängberg, I.,
691 Lindqvist, O., Pirrone, N., Sprovieri, F., Pesenti, E., & Strömberg, D. (2003). Evasion of
692 mercury from coastal and open waters of the Atlantic Ocean and the Mediterranean Sea.
693 *Atmospheric Environment*, *37*, 73–84. https://doi.org/10.1016/S1352-2310(03)00238-3
694 Gérard, J., & Nehmé, C. (2020). Lebanon. *Méditerranée. Revue Géographique Des Pays*
695 *Méditerranéens / Journal of Mediterranean Geography*, *131*, Article 131.
696 https://journals.openedition.org/mediterranee/11018#
697 Giesler, R., Clemmensen, K. E., Wardle, D. A., Klaminder, J., & Bindler, R. (2017). Boreal
698 Forests Sequester Large Amounts of Mercury over Millennial Time Scales in the
699 Absence of Wildfire. *Environmental Science & Technology*, *51*(5), 2621–2627.
700 https://doi.org/10.1021/acs.est.6b06369
701 Grigal, D. (2003). Mercury Sequestration in Forests and Peatlands: A Review. *Journal of*
702 *Environmental Quality - J ENVIRON QUAL*, *32*. https://doi.org/10.2134/jeq2003.0393
703 Guarino, F., Improta, G., Triassi, M., Castiglione, S., & Cicatelli, A. (2021). Air quality
704 biomonitoring through Olea europaea L.: The study case of "Land of pyres."
705 *Chemosphere*, *282*, 131052. https://doi.org/10.1016/j.chemosphere.2021.131052
706 Gworek, B., Dmuchowski, W., & Baczewska-Dąbrowska, A. H. (2020). Mercury in the
707 terrestrial environment: A review. *Environmental Sciences Europe*, *32*(1), 128.
708 https://doi.org/10.1186/s12302-020-00401-x
709 Hanson, P. J., Lindberg, S. E., Tabberer, T. A., Owens, J. G., & Kim, K.-H. (1995). Foliar
710 exchange of mercury vapor: Evidence for a compensation point. *Water, Air, & Soil*
711 *Pollution*, *80*(1–4), 373–382. https://doi.org/10.1007/BF01189687

Higueras, P., Amorós, J. A., Esbrí, J. M., García-Navarro, F. J., Pérez de los Reyes, C., & Moreno, G. (2012). Time and space variations in mercury and other trace element contents in olive tree leaves from the Almadén Hg-mining district. *Journal of Geochemical Exploration*, *123*, 143–151. https://doi.org/10.1016/j.gexplo.2012.04.012

Higueras, P. L., Amorós, J. Á., Esbrí, J. M., Pérez-de-los-Reyes, C., López-Berdonces, M. A., & García-Navarro, F. J. (2016). Mercury transfer from soil to olive trees. A comparison of three different contaminated sites. *Environmental Science and Pollution Research*, *23*(7), 6055–6061. https://doi.org/10.1007/s11356-015-4357-2

Horowitz, H. M., Jacob, D. J., Zhang, Y., Dibble, T. S., Slemr, F., Amos, H. M., Schmidt, J. A., Corbitt, E. S., Marais, E. A., & Sunderland, E. M. (2017). A new mechanism for atmospheric mercury redox chemistry: Implications for the global mercury budget. *Atmospheric Chemistry and Physics*, *17*(10), 6353–6371. https://doi.org/10.5194/acp-17-6353-2017

Jindrich Petrlik, Kodeih, N., IndyACT, Arnika Association, & IPEN WG. (2013). *Mercury in Fish and Hair Samples from Batroun, Lebanon*. https://doi.org/10.13140/RG.2.2.12052.40327

Jiskra, M., Sonke, J. E., Obrist, D., Bieser, J., Ebinghaus, R., Myhre, C. L., Pfaffhuber, K. A., Wängberg, I., Kyllönen, K., Worthy, D., Martin, L. G., Labuschagne, C., Mkololo, T., Ramonet, M., Magand, O., & Dommergue, A. (2018). A vegetation control on seasonal variations in global atmospheric mercury concentrations. *Nature Geoscience*, *11*(4), 244–250. https://doi.org/10.1038/s41561-018-0078-8

Johnson, & Lindberg. (1995). The biogeochemical cycling of Hg in forests: Alternative methods for quantifying total deposition and soil emission. *1995, 80: 1069–1077*, 9.

735 Jurdi, M., Korfali, S. I., Karahagopian, Y., & Davies, B. E. (2002). *Evaluation of Water Quality*
736 *of the Qaraaoun Reservoir, Lebanon: Suitability for Multipurpose Usage*. *77*(11–30), 20.
737 Kabata-Pendias, A., & Pendias, H. (2000). *Trace elements in soils and plants* (3rd ed). CRC
738 Press.
739 Khadari, B., El Bakkali, A., Essalouh, L., Tollon, C., Pinatel, C., & Besnard, G. (2019).
740 Cultivated Olive Diversification at Local and Regional Scales: Evidence From the
741 Genetic Characterization of French Genetic Resources. *Frontiers in Plant Science*, *10*.
742 https://www.frontiersin.org/articles/10.3389/fpls.2019.01593
743 Kobrossi, R., Nuwayhid, I., Sibai, A. M., El-Fadel, M., & Khogali, M. (2002). Respiratory health
744 effects of industrial air pollution on children in North Lebanon. *International Journal of*
745 *Environmental Health Research*, *12*(3), 205–220.
746 https://doi.org/10.1080/09603/202/000000970
747 Kotnik, J., Sprovieri, F., Ogrinc, N., Horvat, M., & Pirrone, N. (2014). Mercury in the
748 Mediterranean, part I: Spatial and temporal trends. *Environmental Science and Pollution*
749 *Research*, *21*(6), 4063–4080. https://doi.org/10.1007/s11356-013-2378-2
750 Labdaoui, D., Lotmani, B., & Aguedal, H. (2021). Assessment of Metal Pollution on the
751 Cultivation of Olive Trees in the Petrochemical Industrial Zone of Arzew (Algeria).
752 *South Asian Journal of Experimental Biology*, *11*(3), Article 3.
753 https://doi.org/10.38150/sajeb.11(3).p227-233
754 *Lebanon: Air Pollution | IAMAT*. (2020). https://www.iamat.org/country/lebanon/risk/air-
755 pollution
756 Li, D., Fang, K., Li, Y., Chen, D., Liu, X., Dong, Z., Zhou, F., Guo, G., Shi, F., Xu, C., & Li, Y.
757 (2017). Climate, intrinsic water-use efficiency and tree growth over the past 150 years in

humid subtropical China. *PLOS ONE*, *12*(2), e0172045. https://doi.org/10.1371/journal.pone.0172045

Li, R., Wu, H., Ding, J., Fu, W., Gan, L., & Li, Y. (2017). Mercury pollution in vegetables, grains and soils from areas surrounding coal-fired power plants. *Scientific Reports*, *7*(1), 46545. https://doi.org/10.1038/srep46545

Lindberg, S., Bullock, R., Ebinghaus, R., Engstrom, D., Feng, X., Fitzgerald, W., Pirrone, N., Prestbo, E., & Seigneur, C. (2007). A Synthesis of Progress and Uncertainties in Attributing the Sources of Mercury in Deposition. *Ambio*, *36*(1), 19–32.

Lindberg, S. E., Jackson, D. R., Huckabee, J. W., Janzen, S. A., Levin, M. J., & Lund, J. R. (1979). Atmospheric Emission and Plant Uptake of Mercury from Agricultural Soils near the Almadén Mercury Mine. *Journal of Environmental Quality*, *8*(4), 572–578. https://doi.org/10.2134/jeq1979.00472425000800040026x

Lodenius, M., Tulisalo, E., & Soltanpour-Gargari, A. (2003). Exchange of mercury between atmosphere and vegetation under contaminated conditions. *Science of The Total Environment*, *304*(1–3), 169–174. https://doi.org/10.1016/S0048-9697(02)00566-1

Luo, Y., Duan, L., Driscoll, C. T., Xu, G., Shao, M., Taylor, M., Wang, S., & Hao, J. (2016). Foliage/atmosphere exchange of mercury in a subtropical coniferous forest in south China. *Journal of Geophysical Research: Biogeosciences*, *121*(7), 2006–2016. https://doi.org/10.1002/2016JG003388

Maillard, F., Girardclos, O., Assad, M., Zappelini, C., Pérez Mena, J. M., Yung, L., Guyeux, C., Chrétien, S., Bigham, G., Cosio, C., & Chalot, M. (2016). Dendrochemical assessment of mercury releases from a pond and dredged-sediment landfill impacted by a chlor-alkali

plant. *Environmental Research*, *148*, 122–126. https://doi.org/10.1016/j.envres.2016.03.034

Martino, M., Tassone, A., Angiuli, L., Naccarato, A., Dambruoso, P. R., Mazzone, F., Trizio, L., Leonardi, C., Petracchini, F., Sprovieri, F., Pirrone, N., D'Amore, F., & Bencardino, M. (2022). First atmospheric mercury measurements at a coastal site in the Apulia region: Seasonal variability and source analysis. *Environmental Science and Pollution Research*, *29*(45), 68460–68475. https://doi.org/10.1007/s11356-022-20505-6

McLagan, D. S., Biester, H., Navrátil, T., Kraemer, S. M., & Schwab, L. (2022). *Internal tree cycling and atmospheric archiving of mercury: Examination with concentration and stable isotope analyses* [Preprint]. Biogeochemistry: Air - Land Exchange. https://doi.org/10.5194/bg-2022-124

McLagan, D. S., Stupple, G. W., Darlington, A., Hayden, K., Steffen, A., & Kamp, L. (2021). Where there is smoke there is mercury: Assessing boreal forest fire mercury emissions using aircraft and highlighting uncertainties associated with upscaling emissions estimates. *Atmos. Chem. Phys.*, 19.

Meddad-Hamza, A., Hamza, N., Neffar, S., Beddiar, A., Gianinazzi, S., & Chenchouni, H. (2017). Spatiotemporal variation of arbuscular mycorrhizal fungal colonization in olive (Olea europaea L.) roots across a broad mesic-xeric climatic gradient in North Africa. *Science of The Total Environment*, *583*, 176–189. https://doi.org/10.1016/j.scitotenv.2017.01.049

Naharro, R., Esbri, J., Amorós, J., & Higueras, P. (2018). *Atmospheric mercury uptake and desorption from olive-tree leaves*. *20*(EGU2018-2982,2018), 2.

Nassif, N., Jaoude, L. A., El Hage, M., & Robinson, C. A. (2016). Data Exploration and Reconnaissance to Identify Ocean Phenomena: A Guide for InSitu Data Collection. *Journal of Water Resource and Protection*, *08*(10), 929–943. https://doi.org/10.4236/jwarp.2016.810076

Niu, Z., Zhang, X., Wang, Z., & Ci, Z. (2011). Field controlled experiments of mercury accumulation in crops from air and soil. *Environmental Pollution*, *159*(10), 2684–2689. https://doi.org/10.1016/j.envpol.2011.05.029

Obrist, D. (2007). Atmospheric mercury pollution due to losses of terrestrial carbon pools? *Biogeochemistry*, *85*(2), 119–123. https://doi.org/10.1007/s10533-007-9108-0

Obrist, D., Johnson, D. W., & Lindberg, S. E. (2009). *Mercury concentrations and pools in four Sierra Nevada forest sites, and relationships to organic carbon and nitrogen*. 13.

Obrist, D., Kirk, J. L., Zhang, L., Sunderland, E. M., Jiskra, M., & Selin, N. E. (2018). A review of global environmental mercury processes in response to human and natural perturbations: Changes of emissions, climate, and land use. *Ambio*, *47*(2), 116–140. https://doi.org/10.1007/s13280-017-1004-9

Obrist, M. K., Rathey, E., Bontadina, F., Martinoli, A., Conedera, M., Christe, P., & Moretti, M. (2011). Response of bat species to sylvo-pastoral abandonment. *Forest Ecology and Management*, *261*(3), 789–798. https://doi.org/10.1016/j.foreco.2010.12.010

O'Connor, D., Hou, D., Ok, Y. S., Mulder, J., Duan, L., Wu, Q., Wang, S., Tack, F. M. G., & Rinklebe, J. (2019). Mercury speciation, transformation, and transportation in soils, atmospheric flux, and implications for risk management: A critical review. *Environment International*, *126*, 747–761. https://doi.org/10.1016/j.envint.2019.03.019

824 Ozturk, M., Altay, V., Gönenç, T. M., Unal, B. T., Efe, R., Akçiçek, E., & Bukhari, A. (2021).
825 An Overview of Olive Cultivation in Turkey: Botanical Features, Eco-Physiology and
826 Phytochemical Aspects. *Agronomy*, *11*(2), 295.
827 https://doi.org/10.3390/agronomy11020295
828 Patra, M., & Sharma, A. (2000). Mercury toxicity in plants. *The Botanical Review*, *66*(3), 379–
829 422. https://doi.org/10.1007/BF02868923
830 Pleijel, H., Klingberg, J., Nerentorp, M., Broberg, M. C., Nyirambangutse, B., Munthe, J., &
831 Wallin, G. (2021). *Mercury accumulation in leaves of different plant types – the*
832 *significance of tissue age and specific leaf area* [Preprint]. Biogeochemistry: Air - Land
833 Exchange. https://doi.org/10.5194/bg-2021-117
834 Pokharel, A. K., & Obrist, D. (2011). Fate of mercury in tree litter during decomposition.
835 *Biogeosciences*, *8*(9), 2507–2521. https://doi.org/10.5194/bg-8-2507-2011
836 Proietti, P., & Famiani, F. (2002). Diurnal and Seasonal Changes in Photosynthetic
837 Characteristics in Different Olive (Olea europaea L.) Cultivars. *Photosynthetica*, *40*(2),
838 171–176. https://doi.org/10.1023/A:1021329220613
839 Rea, A. W., Keeler, G. J., & Scherbatskoy, T. (1996). The deposition of mercury in throughfall
840 and litterfall in the lake champlain watershed: A short-term study. *Atmospheric*
841 *Environment*, *30*(19), 3257–3263. https://doi.org/10.1016/1352-2310(96)00087-8
842 Rea, A. W., Lindberg, S. E., Scherbatskoy, T., & Keeler, G. J. (2002). *Mercury Accumulation in*
843 *Foliage over Time in Two Northern Mixed-Hardwood Forests*. 19.
844 Riaz, M., Kamran, M., Fang, Y., Wang, Q., Cao, H., Yang, G., Deng, L., Wang, Y., Zhou, Y.,
845 Anastopoulos, I., & Wang, X. (2021). Arbuscular mycorrhizal fungi-induced mitigation

of heavy metal phytotoxicity in metal contaminated soils: A critical review. *Journal of Hazardous Materials*, *402*, 123919. https://doi.org/10.1016/j.jhazmat.2020.123919

Richardson, J. B., Friedland, A. J., Engerbretson, T. R., Kaste, J. M., & Jackson, B. P. (2013). Spatial and vertical distribution of mercury in upland forest soils across the northeastern United States. *Environmental Pollution (Barking, Essex : 1987)*, *182*, 127–134. https://doi.org/10.1016/j.envpol.2013.07.011

Sanz-Cortés, F., Martinez-Calvo, J., Badenes, M. L., Bleiholder, H., Hack, H., Llacer, G., & Meier, U. (2002). Phenological growth stages of olive trees (Olea europaea). *Annals of Applied Biology*, *140*(2), 151–157. https://doi.org/10.1111/j.1744-7348.2002.tb00167.x

Schaefer, K., Elshorbany, Y., Jafarov, E., Schuster, P. F., Striegl, R. G., Wickland, K. P., & Sunderland, E. M. (2020). Potential impacts of mercury released from thawing permafrost. *Nature Communications*, *11*(1), Article 1. https://doi.org/10.1038/s41467-020-18398-5

Schneider, L., Allen, K., Walker, M., Morgan, C., & Haberle, S. (2019). Using Tree Rings to Track Atmospheric Mercury Pollution in Australia: The Legacy of Mining in Tasmania. *Environmental Science & Technology*, *53*(10), 5697–5706. https://doi.org/10.1021/acs.est.8b06712

Schwesig, D., & Krebs, O. (2003). The role of ground vegetation in the uptake of mercury and methylmercury in a forest ecosystem. *Plant and Soil*, 11.

Senesil, G. S., Baldassarre, G., Senesi, N., & Radina, B. (1999). Trace element inputs into soils by anthropogenic activities and implications for human health. *Chemosphere*, *39*(2), 343–377. https://doi.org/10.1016/S0045-6535(99)00115-0

Sghaier, A., Perttunen, J., Sievaènen, R., Boujnah, D., Ouessar, M., Ben Ayed, R., & Naggaz, K. (2019). Photosynthetical activity modelisation of olive trees growing under drought conditions. *Scientific Reports*, *9*(1), 15536. https://doi.org/10.1038/s41598-019-52094-9

Siudek, P., Kurzyca, I., & Siepak, J. (2016). Atmospheric deposition of mercury in central Poland: Sources and seasonal trends. *Atmospheric Research*, *170*, 14–22. https://doi.org/10.1016/j.atmosres.2015.11.004

Teixeira, D. C., Lacerda, L. D., & Silva-Filho, E. V. (2017). Mercury sequestration by rainforests: The influence of microclimate and different successional stages. *Chemosphere*, *168*, 1186–1193. https://doi.org/10.1016/j.chemosphere.2016.10.081

Terral, J.-F., Alonso, N., Capdevila, R. B. i, Chatti, N., Fabre, L., Fiorentino, G., Marinval, P., Jordá, G. P., Pradat, B., Rovira, N., & Alibert, P. (2004). Historical biogeography of olive domestication (Olea europaea L.) as revealed by geometrical morphometry applied to biological and archaeological material: Historical biogeography of olive domestication (Olea europaea L.). *Journal of Biogeography*, *31*(1), 63–77. https://doi.org/10.1046/j.0305-0270.2003.01019.x

Tomiyasu, T., Matsuo, T., Miyamoto, J., Imura, R., Anazawa, K., & Sakamoto, H. (2005). Low level mercury uptake by plants from natural environments—Mercury distribution in Solidago altissima L.-. *Environmental Sciences: An International Journal of Environmental Physiology and Toxicology*, *12*(4), 231–238.

UNEP. (2019). *Technical Background Report to the Global Mercury Assessment 2018*. IVL Svenska Miljöinstitutet.

Wang, X., Lin, C.-J., Lu, Z., Zhang, H., Zhang, Y., & Feng, X. (2016). Enhanced accumulation and storage of mercury on subtropical evergreen forest floor: Implications on mercury

budget in global forest ecosystems: HG STORAGE ON SUBTROPICAL FOREST FLOOR. *Journal of Geophysical Research: Biogeosciences*, *121*(8), 2096–2109. https://doi.org/10.1002/2016JG003446

Wängberg, I., Munthe, J., Pirrone, N., Iverfeldt, Å., Bahlman, E., Costa, P., Ebinghaus, R., Feng, X., Ferrara, R., Gårdfeldt, K., Kock, H., Lanzillotta, E., Mamane, Y., Mas, F., Melamed, E., Osnat, Y., Prestbo, E., Sommar, J., Schmolke, S., … Tuncel, G. (2001). Atmospheric mercury distribution in Northern Europe and in the Mediterranean region. *Atmospheric Environment*, *35*(17), 3019–3025. https://doi.org/10.1016/S1352-2310(01)00105-4

Weigelt, A., Ebinghaus, R., Manning, A. J., Derwent, R. G., Simmonds, P. G., Spain, T. G., Jennings, S. G., & Slemr, F. (2015). Analysis and interpretation of 18 years of mercury observations since 1996 at Mace Head, Ireland. *Atmospheric Environment*, *100*, 85–93. https://doi.org/10.1016/j.atmosenv.2014.10.050

Wofsy, S. C., Goulden, M. L., Munger, J. W., Fan, S.-M., Bakwin, P. S., Daube, B. C., Bassow, S. L., & Bazzaz, F. A. (1993). Net Exchange of CO_2 in a Mid-Latitude Forest. *Science*, *260*(5112), 1314–1317. https://doi.org/10.1126/science.260.5112.1314

Wohlgemuth, L., Rautio, P., Ahrends, B., Russ, A., Vesterdal, L., Waldner, P., Timmermann, V., Eickenscheidt, N., Fürst, A., Greve, M., Roskams, P., Thimonier, A., Nicolas, M., Kowalska, A., Ingerslev, M., Merilä, P., Benham, S., Iacoban, C., Hoch, G., … Jiskra, M. (2021). *Physiological and climate controls on foliar mercury uptake by European tree species* [Preprint]. Biogeochemistry: Air - Land Exchange. https://doi.org/10.5194/bg-2021-239

912 Wright, L. P., Zhang, L., & Marsik, F. J. (2016). Overview of mercury dry deposition, litterfall,
913 and throughfall studies. *Atmospheric Chemistry and Physics*, *16*(21), 13399–13416.
914 https://doi.org/10.5194/acp-16-13399-2016
915 Wu, S., Zhang, X., Chen, B., Wu, Z., Li, T., Hu, Y., Sun, Y., & Wang, Y. (2016). Chromium
916 immobilization by extraradical mycelium of arbuscular mycorrhiza contributes to plant
917 chromium tolerance. *Environmental and Experimental Botany*, *122*, 10–18.
918 https://doi.org/10.1016/j.envexpbot.2015.08.006
919 Yammine, P., Kfoury, A., El-Khoury, B., Nouali, H., El-Nakat, H., Ledoux, F., Courcot, D., &
920 Aboukaïs, A. (2010). A preliminary evaluation of the inorganic chemical composition of
921 atmospheric tsp in the selaata region, north lebanon. *Lebanese Science Journal*, *11*(1), 18.
922 Yanai, R. D., Yang, Y., Wild, A. D., Smith, K. T., & Driscoll, C. T. (2020). New Approaches to
923 Understand Mercury in Trees: Radial and Longitudinal Patterns of Mercury in Tree Rings
924 and Genetic Control of Mercury in Maple Sap. *Water, Air, & Soil Pollution*, *231*(5), 248.
925 https://doi.org/10.1007/s11270-020-04601-2
926 Yang, Y., Yanai, R. D., Driscoll, C. T., Montesdeoca, M., & Smith, K. T. (2018). Concentrations
927 and content of mercury in bark, wood, and leaves in hardwoods and conifers in four
928 forested sites in the northeastern USA. *PLOS ONE*, *13*(4), e0196293.
929 https://doi.org/10.1371/journal.pone.0196293
930 Yazbeck, E. B., Rizk, G. A., Hassoun, G., El-Khoury, R., & Geagea, L. (2018). *Ecological*
931 *characterization of ancient olive trees in Lebanon- Bshaaleh area and their age*
932 *estimation*. *11*(2 Ver. 1), 35–44.
933 Zhao, X., & Wang, D. (2010). Mercury in some chemical fertilizers and the effect of calcium
934 superphosphate on mercury uptake by corn seedlings (Zea mays L.). *Journal of*

Environmental Sciences, *22*(8), 1184–1188. https://doi.org/10.1016/S1001-0742(09)60236-9

Zhou, J., Obrist, D., Dastoor, A., Jiskra, M., & Ryjkov, A. (2021). Vegetation uptake of mercury and impacts on global cycling. *Nature Reviews Earth & Environment*, *2*(4), 269–284. https://doi.org/10.1038/s43017-021-00146-y

Zhou, J., Wang, Z., & Zhang, X. (2018). Deposition and Fate of Mercury in Litterfall, Litter, and Soil in Coniferous and Broad-Leaved Forests. *Journal of Geophysical Research: Biogeosciences*, *123*(8), 2590–2603. https://doi.org/10.1029/2018JG004415